Are recent water models obtained by fitting diffraction data consistent with infrared/Raman and x-ray absorption spectra?

ARTICLE *in* THE JOURNAL OF CHEMICAL PHYSICS · JANUARY 2007

Impact Factor: 2.95 · DOI: 10.1063/1.2408419 · Source: PubMed

Are recent water models obtained by fitting diffraction data consistent with infrared/Raman and x-ray absorption spectra?

Mikael Leetmaa and Mathias Ljungberg
Fysikum, AlbaNova, Stockholm University, SE-106 91 Stockholm, Sweden

Hirohito Ogasawara
Stanford Synchrotron Radiation Laboratory, P.O. Box 20450, Stanford, California 94309

Michael Odelius
Fysikum, AlbaNova, Stockholm University, SE-106 91 Stockholm, Sweden

Lars-Åke Näslund and Anders Nilsson
Fysikum, AlbaNova, Stockholm University, SE-106 91 Stockholm, Sweden
and Stanford Synchrotron Radiation Laboratory, P.O. Box 20450, Stanford, California 94309

Lars G. M. Pettersson
Fysikum, AlbaNova, Stockholm University, SE-106 91 Stockholm, Sweden

(Received 24 July 2006; accepted 17 November 2006; published online 29 December 2006)

X-ray absorption (XA) spectra have been computed based on water structures obtained from a recent fit to x-ray and neutron diffraction data using models ranging from symmetrical to asymmetrical local coordination of the water molecules [A. K. Soper, J. Phys.: Condens. Matter **17**, S3273 (2005)]. It is found that both the obtained symmetric and asymmetric structural models of water give similar looking XA spectra, which do not match the experiment. The fitted models both contain unphysical structures that are allowed by the diffraction data, where, e.g., hydrogen-hydrogen interactions may occur. A modification to the asymmetric model, in which the non-hydrogen-bonded OH intramolecular distance is allowed to become shorter while the bonded OH distance becomes longer, improves the situation somewhat, but the overall agreement is still unsatisfactory. The electric field (E-field) distributions and infrared (IR) spectra are also calculated using two established theoretical approaches, which, however, show significant discrepancies in their predictions for the asymmetric structural models. Both approaches predict the Raman spectrum of the symmetric model fitted to the diffraction data to be significantly blueshifted compared to experiment. At the moment no water model exists that can equally well describe IR/Raman, x-ray absorption spectroscopy, and diffraction data. © *2006 American Institute of Physics*. [DOI: 10.1063/1.2408419]

INTRODUCTION

In a recent study[1] the available neutron- and x-ray diffraction data on water under ambient conditions were reanalyzed using empirical potential structure refinement (EPSR) in terms of both a symmetrical and a series of asymmetrical potential models for the water-water interaction with the surprising result that all the investigated models could be made to represent the data to a seemingly equivalent level of fitting. This investigation was inspired by the substantial debate[2–12] around the paper by Wernet *et al.*[13] giving experimental x-ray absorption spectroscopy (XAS) and x-ray Raman scattering (XRS) evidence for a predominantly asymmetric hydrogen-bond (H-bond) coordination in liquid water. The conclusion that, on the average, the molecules in the liquid only have slightly more than two strong H-bonds challenges the textbook picture of the liquid, as having closer to four strong bonds.

The traditional view of water goes back at least more than 70 years to the work of Bernal and Fowler[14] who successfully analyzed the existing x-ray diffraction data on water in terms of a disordered quartz-like structure. These ideas were reinforced in subsequent analyses[15] and became embedded in many of the early computer simulations of water[16] and much of the work that has followed since. It is important to note here that even with the asymmetric models of Ref. 1 the first neighbor *coordination* number of water does not change appreciably from its traditional value of 4+. What changes between the different models is the number of strong hydrogen bonds, as classified by the criterion of Wernet *et al.*[13] It should also be pointed out that no intermolecular water potential has yet been constructed which successfully reproduces the asymmetry described by Wernet *et al.* and the XA data. In fact, no theoretical simulation model has been constructed that simultaneously reproduces all other known properties such as the melting, boiling and critical point, the temperature of maximum density, the anomalous pressure dependence of dynamic quantities such as the diffusion coefficient, and the experimental radial distribution functions of water, even in a qualitative sense although present models typically are successful in describing subsets of these properties.[17]

Water is ubiquitous and is a fundamental component in

all biological, geochemical, etc. systems and is the basis for all aqueous solution chemistry. Knowledge of its structure and detailed properties and how these are affected by, e.g., solutes, *p*H, temperature, and pressure is of fundamental importance, as is the ability to reproduce them using theoretical simulation techniques. The radial distribution functions from diffraction experiments provide important calibration points for the simulations, and it is of great importance to establish their accuracy and limitations. However, some confusion seems to exist in the literature with different sets of experimental x-ray diffraction data published by the same group and also as to their normalization.[10,18,19] Furthermore, a recent comparison[10] of the EPSR fitted structural models from Ref. 1 with x-ray diffraction data exaggerates the difference between fitted and experimental data for the asymmetrical structural model through a plotting mistake.[20] When correctly plotted, the agreement between the model and experiment is such that it is usually accepted as within the error bars. In view of this and the present debate around the structure of liquid water, recent, substantially more extended, x-ray diffraction data may help clarify the situation.[21]

Recent *ab initio* studies of water[22] using density functional methods have furthermore demonstrated the significant sensitivity of water structure and dynamics to the particular choice of density functional in the simulation, and there is no clear answer to this problem at present, although none of these studies challenge the concept of water as a tetrahedral liquid.[4] In addition the importance of quantum effects has been established.[23]

In the fits described in Ref. 1 asymmetry in the local water environment was introduced by using an increasingly asymmetric charge distribution on the water molecule. Starting from a symmetric distribution of charge between the two water hydrogens, the end point was a situation where all the charge was on one hydrogen atom with zero charge on the other; this should not at all be viewed as a representation of the actual charge distribution in the liquid, as incorrectly assumed in Ref. 10, but rather as a way to generate a series of examples of asymmetrical structures.

In the fits it was found that with the perturbation to the starting potential found by EPSR, all of these models could be made to give a reasonable set of structure factors consistent with all the diffraction data. The fits were not perfect, but the discrepancies were sufficiently small in all cases that it was concluded that all the investigated models could represent the diffraction data; later work has led to this conclusion being questioned however (A. K. Soper, private communication). Essentially, what happens in these asymmetric models compared to the symmetric model investigated is that changes induced in the coordination in one hydrogen shell by the lack of charge symmetry are offset by opposing changes in the coordination in the other hydrogen shell, leaving the average angularly integrated coordination relatively unchanged compared to the symmetric model.

This investigation raises the question, given that it is postulated on the basis of the XA data that the local structure of water is predominantly asymmetric, whether or not the asymmetric structural solutions found from the new analysis are compatible with the experimental XAS/XRS data as well as available infrared (IR) and Raman spectroscopy data. In short, are the particular asymmetric models obtained in Ref. 1 valid models for the liquid also in the sense of the XA and IR/Raman spectra? Furthermore, although it has been shown by Wernet *et al.*[13] and Odelius *et al.*[12] that a symmetrical model cannot describe XAS, a second question is whether the obtained symmetrical model is consistent with IR/Raman spectra.

TABLE I. Characterization of water molecular models used in the EPSR refinement in Ref. 1. *Q* gives the charge of the species and HB gives the resulting average number of H-bonds using the definition of Ref. 13.

Model	*Q*(O)	*Q*(H1)	*Q*(H2)	HB
*a*2	−0.848	+0.424	+0.424	2.9
*a*2_2	−0.810	+0.262	+0.548	2.6
*a*2_3	−0.785	+0.207	+0.578	2.5
*a*2_4	−0.680	+0.100	+0.580	2.3
*a*2_6	−0.600	+0.000	+0.600	2.2

In the present work we present results from an extensive study calculating theoretical XA spectra and analyzing IR/Raman spectra for the liquid water structures generated in Ref. 1 by fitting to the diffraction data. We focus on the two extreme models, i.e., symmetric with equivalent hydrogen atoms giving 2.9 H-bonds per molecule in the EPSR fit and the most asymmetric situation having an average of 2.2-H bonds per molecule. We find that neither model can correctly reproduce the XA spectra and furthermore report a strong discrepancy for the asymmetric model between two different published techniques to predict the Raman and IR spectra. Both the symmetric and asymmetric structural models, as fitted to the diffraction data, are found to contain unphysical aspects to varying degree where, e.g., hydrogen atoms on neighboring molecules point towards each other which is not expected based on simple rules regarding hydrogen bonding.

METHODS

XA spectrum calculations

Statistics of the number of H-bonds according to the geometrical cone criterion in Ref. 13 was extracted from the symmetric (*a*2), the completely asymmetric (*a*2_6), and less asymmetric (*a*2_4) dumps from Ref. 1 with the characteristics of the different models summarized in Table I. Out of the 1800 molecules in each dump, between 200 and 300 molecules were selected randomly for XA spectrum calculations according to the H-bond statistics. The spectrum calculations were performed using cluster models where the closest 31 neighboring waters to the central water were retained to form computational models consisting of 32 water molecules.

All XA spectrum calculations were performed using the STOBE-DEMON code[24] with the half core-hole transition potential method.[25] The unoccupied states were determined in a double-basis-set procedure where, after convergence, the basis set was augmented with a large, diffuse basis set to better describe Rydberg and continuum states.[25,26] The computational procedure has been described in detail elsewhere.[25,27]

Hydrogen was described using the standard (311/1) basis set of Huzinaga,[28] while the central core-excited oxygen was described using the core extended IGLO-III basis set of Kutzelnigg *et al.*[29] which allows for core relaxation effects. The remaining oxygens were described using effective core potentials[30] (ECPs) in conjunction with a (311/211) basis set for the valence electrons. The ECPs have no significant effect on the final XA spectrum but were used to simplify the calculations by guaranteeing core-hole localization on the central oxygen. The auxiliary basis sets used were (4,4;4,4) for oxygen and (3,1;3,1) for hydrogen where the nomenclature $[N_C(s), N_C(spd); N_{xc}(s), N_{xc}(spd)]$ indicates the number of *s* and *spd* functions used to fit the Coulomb and exchange correlation potentials, respectively. For all calculations the gradient-corrected exchange functional of Becke[31] was used together with the correlation functional of Perdew and Wang.[32]

In order to get the calculated spectra on an absolute energy scale, a ΔKohn-Sham (ΔKS) energy correction calculation was performed for each individual cluster.[27] The total energy of the first core-excited state was computed by placing an electron in the lowest unoccupied molecular orbital (LUMO) in the presence of the core-hole, allowing for full relaxation of the orbitals. The energy position of the first peak in the transition-potential XA spectrum was set equal to the total energy difference between the ground state and the core-excited state; all other peaks were shifted accordingly.

The limited cluster size may give rise to surface states as an artifact, not present in the spectrum when going to larger clusters. These states, if present, show up as extra peaks with low oscillator strength, somewhat lower in energy than the real spectrum onset energy. When using smaller clusters, the procedure of augmenting the basis with the diffuse functions may give rise to additional surface states not appearing when using only the smaller basis. On shifting the spectra precautions have to be taken in order not to shift a peak corresponding to some surface state generated by the augmentation basis but rather the peak corresponding to the first core-excited state, whether it may be a surface state or not, to the calculated ΔKS energy. XA spectra for some different clusters from the asymmetric dump were recalculated without the diffuse functions. Comparison with the corresponding spectra and orbitals obtained using the augmentation basis did not reveal any significant discrepancies in the energy region of interest. In the cases where there were obvious surface states in the spectrum they appeared in both basis set descriptions, thus without having impact on the ΔKS shifting procedure.

Relativistic- and functional-dependent shifts were added to all spectra to correct for deficiencies due to the functional and basis set in describing mainly the core level.[33] The computed core-electron binding energy for the oxygen 1*s* level in gas-phase water (539.1 eV) was compared to the experimental gas-phase value (539.8 eV),[34] giving an empirical shift of +0.7 eV; 0.33 eV of this shift is due to relativistic effects.[33]

To facilitate comparison with experimental data all discrete spectra were convoluted using Gaussian broadening with a full width at half maximum (FWHM) of 0.5 eV up to 536.0 eV. The broadening was then linearly increased to 4.25 eV at 548.0 eV after which a constant broadening of 4.25 eV was used. The broadening mimics lifetime effects, vibrational excitations, and instrumental resolution as well as compensates for the limited sampling performed in the continuum due to the finite size of the augmentation basis (~150 functions). A rather large (4.25 eV) broadening in the continuum is applied to ensure that spurious, basis set related states do not affect the spectrum. In Ref. 12 we have compared the present broadening scheme with a constant broadening of all states by 0.5 eV before summation and have shown that the spectra are very similar. The applied procedure leads to a good representation of the near-edge region of interest and a smoother and still properly normalized continuum where true continuum resonances are unaffected by the broadening while isolated, basis set related spurious states are suppressed.

EPSR refinement

Much of the details of the EPSR refinement used in this work have already been given in the preceding paper[1] and will not be repeated here. In that work the water molecule atoms were labeled OW for oxygen and HW1 and HW2 for the two hydrogen atoms. The only adjustment to the procedure compared to that used previously was that for the fully asymmetric model, on the assumption that one hydrogen, HW1, is mostly not hydrogen bonded, while the other, HW2, is, this should also affect the respective OW–HW1 and OW–HW2 bond lengths, since these are known to lengthen slightly with increased hydrogen bonding. Since the water molecule in the liquid has an average O–H bond length of 0.98 Å, whereas in the gas phase the O–H bond length is 0.9572 Å,[35] for the revised simulations the OW–HW1 (zero charge) bond length was set to 0.96 Å, while the bonded hydrogen atom bond length, OW–HW2, was set to 1.00 Å. At the same time the force constants for these two distances were adjusted so that the rms standard deviation on OW–HW1 was 0.054 Å, while that on OW–HW2 was 0.094 Å, giving a mean value and rms standard deviation for the O–H bond of 0.98 Å and 0.074 Å respectively, in keeping with the neutron diffraction data. The fits to the diffraction data obtained with these revised distances are unchanged compared to those shown previously.[1]

IR/Raman

Two different approaches to estimate the IR/Raman spectra of HOD/D_2O based on the generated structures and the electric field (E-field) from extended simple point charge (SPC/E) charges on each molecule were used in the present work. In the method of Skinner and co-workers[36,37] the spectra are related to the E-field projected along the internal O–H bond through a fit of the E-field versus one-dimensional anharmonic frequencies obtained through quantum chemical calculations of a series of points along the OH stretch. The method assumes no coupling between the OH and OD oscillators and the fit relating E-field to frequency was obtained through calculations on cluster models extracted from molecular dynamics (MD) simulations.[36,37] In the method of Hayashi *et al.*[38] the IR spectrum of a single water molecule (HOD) is calculated *ab initio* for different surroundings of

point charges. Calculated frequencies and transition dipole moments are mapped to a nine component vector consisting of the three components of the electric field and the six independent components of the electric field gradient, all of which are calculated at the center of charge of the molecule. The form of the mapping is a Taylor expansion to second order around the gas phase frequency (or transition dipole moment). As opposed to the approach of Skinner, this method does not depend on a specific potential when mapping frequencies to the field vector which may be assumed to make the method more general. Also the method does not assume a complete decoupling of the O–H stretch. Since only frequencies for a single molecule are calculated, cooperativity effects are not included which can be seen as a (minor) drawback of the method.

When applying the method of Skinner and co-workers, the E-field (in a.u.) from the surrounding water molecules within a predefined cutoff radius (using periodic boundary conditions) was calculated for each internal O–H bond in the dump at a point 0.975 Å from the oxygen, in the direction of the O–H bond. Then the E-field was projected along the direction of the bond in question. The E-field from the solvated water molecule itself was not included. The reason why the E-field was calculated at a fixed distance from the oxygen (and not on the hydrogen atom) was to remove undesired features of the flexible EPSR water model in terms of varying internal bond length. The calculated E-field was found to converge rapidly with increasing cutoff radius, and a radius of 35 Å was found to be sufficient. For easier comparison with experimental spectra, the distributions were broadened by Gaussian convolution using a full width at half maximum (FWHM) corresponding to approximately 75 cm^{-1}. This broadening makes the spectrum/distribution smoother, compensating for the limited statistics obtainable from the single dump. The width, however, is not increased, as can be seen by comparison with the unbroadened spectrum/distribution from a full SPC/E trajectory where the sampling is not an issue (Figs. 5 and 6). The reliability of the broadening was furthermore confirmed by expanding the distribution in a Fourier series retaining only the lower frequency components.

Since a flexible water model was used in the EPSR fits, some precautions should be taken, and a number of different E-field distributions were generated for each dump to investigate the sensitivity to changes in internal geometry. To see the effect of this, all molecules were replaced by SPC/E molecules (O–H distance=1 Å, H–O–H angle 109.47°), in such a way that the new molecule lies in the same plane and faces essentially the same direction as the old one. This was done by defining the orientation of the water molecule using three new basis vectors $v1=(\mathrm{OH1}\times\mathrm{OH2})/|\mathrm{OH1}\times\mathrm{OH2}|$ (where OH1 and OH2 are the vectors from the oxygen to the hydrogen), $v2=(\mathrm{OH1}/|\mathrm{OH1}|+\mathrm{OH2}/|\mathrm{OH2}|)/|\mathrm{OH1}/|\mathrm{OH1}|+\mathrm{OH2}/|\mathrm{OH2}||$, and $v3=v1\times v2$. The rigid SPC/E molecule was then put in this new coordinate system (where $v1$ defines the plane), keeping the angles symmetric about $v2$. SPC/E charges $[Q(\mathrm{O})=-0.8476;\ Q(\mathrm{H})=+0.4238]$ were used throughout.

Using the approach of Hayashi *et al.*, the frequencies and intensities for single structures (snapshots) were calculated according to Eq. (12) and (13) in Ref. 38 using the tabulated values of ω and μ from Tables 7 and 8. The electric field and the electric field gradient were calculated at a point corresponding to the center of charge of a rigid SPC/E molecule. This was done for each water molecule using the same point charges and cutoff as before. The obtained spectrum was also in this case broadened using a Gaussian of 75 cm^{-1} FWHM to make it smoother. In Ref. 38 dynamical information is obtained from MD simulations and used to calculate the line-shape of the IR spectrum. For our purposes, we only use the static distributions since we are mainly interested in the specific structures obtained in Ref. 1.

For specific situations, in cases with strongly negative E-fields, the associated anharmonic frequencies were computed *ab initio* following the approach of Skinner and co-workers;[36,37] this was deemed necessary since the relationship between E-field and frequency has only been investigated earlier for positive E-fields. Clusters of ten water molecules were extracted from the dump by including the molecule in the center and its nine closest neighbor molecules. The potential surface of an (assumed) uncoupled O–H stretch was scanned by doing eight energy calculations along the bond, starting 0.72 Å from the oxygen, with steps of 0.08 Å. The points were then fitted to a Morse potential from which an analytic expression of the energy was obtained. The GAUSSIAN 98 software was used at the B3LYP/6-311++G(d,p) level of theory.[39] We found that the approximate relationship between field and frequency can be extended to negative fields, giving blueshifted frequencies compared to gas phase. In addition, two *ab initio* models, a water hexamer in ring conformation and a seven molecule cluster consisting of two fused tetrameter rings (ditetramer) with the molecule in the middle fully H-bonded were geometry optimized at the same level of theory using the tightest convergence criteria available, and the fully anharmonic frequencies were computed for the case of an HOD molecule in D_2O using the GAUSSIAN 03 implementation of the method of Barone.[40]

RESULTS

The XA spectrum of liquid water (Fig. 1) is characterized by a well-defined preedge at 535 eV, the main edge at 537.6 eV, and a weak postedge around 540–541 eV.[13,41] The preedge has been characterized as due to excitations into a localized O–H intermolecular antibonding state associated with non-H-bonded hydrogens on molecules where the other hydrogen is involved in a strong H-bond.[13,42] The postedge, on the other hand, is due to excitations involving states associated with the H-bonds. The orbitals specifically involved are antibonding with respect to the H-bond as well as antibonding with respect to the intramolecular O–H bond. This makes their energy position a sensitive measure of the H-bond distance such that the distribution of H-bond distances defines both the peak position and width of the postedge peak.[12] In line with these assignments the spectrum of

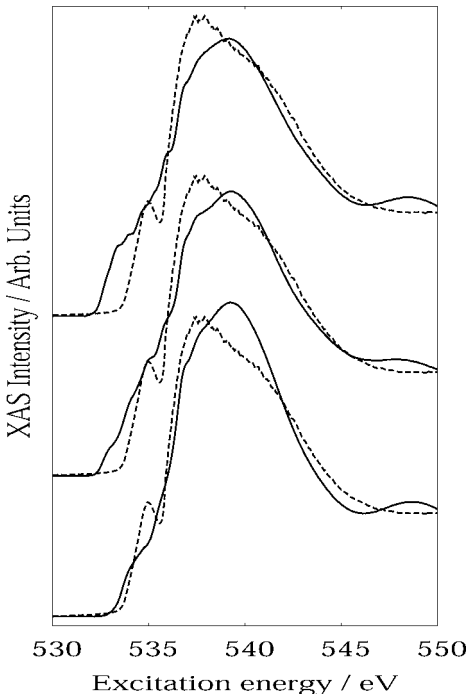

FIG. 1. Comparison of experimental (dashed) (Ref. 6) and computed (full) XA spectra using the symmetric ($a2$, bottom), asymmetric ($a2\_4$, middle), and most asymmetric ($a2\_6$, top) models. The nomenclature for the models is taken from Ref. 1.

bulk ice has only a weak preedge mainly due to proton disorder, internal defects, and remaining surface contributions, while the postedge is well defined.[13]

In Fig. 1 we show a comparison with experiment on liquid water from Ref. 6 and the computed spectra for three of the fitted models from Ref. 1; the symmetrical ($a2$), completely asymmetrical ($a2\_6$), and less asymmetrical ($a2\_4$) models using the notation of Ref. 1. For convenience we summarize the characteristics of the models used in Ref. 1 in Table I. Note that the experimental XA spectrum is taken from Ref. 6 where additional corrections for small remaining saturation effects have been made in comparison with spectra obtained using transmission mode and XRS; the consistency and reproducibility between the three different measurement techniques strongly validate the experimental data.[6]

Beginning with the symmetrical case (Fig. 1, bottom) we find reasonable agreement in terms of the energy position of the onset of the spectrum, but the characteristic features of the liquid XAS spectrum in terms of a well-defined preedge and main-edge and weak postedge are absent in the theoretical spectrum. Instead, the spectrum resembles that of bulk ice with weak preedge and main edge and a dominant postedge at 539 eV which, however, due to the distortions and elongations in the H-bond network is 1.5 eV lower than in ice. Note that this is intermediate between the rather sharp main edge and the true, weak postedge in the liquid which appears as a shoulder around 540.5 eV. This icelike spectrum is similar to spectra computed from MD dumps using classical SPC or Car-Parrinello MD (CPMD) although in the latter cases the postedge appears at a higher energy.[12] Note that the same H-bond criterion applied to the SPC or CPMD structures results in ~3.5 H-bonds rather than the 2.9 obtained in Ref. 1, consistent with the presence of shorter H-bond distances as indicated by the higher energy for the postedge[12] and further demonstrating that the structural models are different in spite of the fact that they give similar shape of the XA spectra. The absence of the preedge and main edge is indicative of too few weakened or broken H bonds in the structural model. This is in agreement with preceding analyses of strongly coordinated water structures from CPMD and classical force-field simulations as well as with experiment on bulk ice.[7,12,13]

The completely asymmetric $a2\_6$ model, on the other hand, shows a redistribution of intensity from the postedge region to lower energies which is what is expected for an asymmetrical structure.[12,13] However, most of the low energy intensity is too low in energy by almost 2 eV. It furthermore does not show the distinct preedge and main edge characteristic of liquid water, and also in this case the postedge appears at 539 eV which is too low compared with experiment. The somewhat less asymmetric case, $a2\_4$, results in an XA spectrum intermediate between the two extremes. The most obvious discrepancy with experiment, in particular for the $a2\_6$ model, is the large intensity found before the onset of the true spectrum which indicates that this particular asymmetrical structure has deficiencies according to the XAS calculations. This is also seen for the symmetrical model $a2$ in Fig. 1, but to a much smaller extent. We note that symmetrical models generated by SPC or CPMD do not show any of these unphysical low energy spectral features observed in the spectrum of the present symmetrical model.[12]

In order to find and analyze the specific local structures contributing to the intensity below the preedge, the intensity was integrated up to the experimental spectrum onset for each of the spectra contributing to the summed spectrum. The structures were then divided into three classes according to the integrated intensity (small, intermediate, large) before the spectrum onset and correlation with various structural parameters was sought. In the symmetrical model the two hydrogens are equivalent, while in the asymmetrical model hydrogen H1 carries zero charge and H2 carries all of the compensating charges relative to the oxygen. The obvious result from the EPSR fit based on this potential is then that H2 is H-bonded while H1 nearly always is free. Since the preedge is due to excitations localized on the non-H-bonded OH1 group and involving the intramolecular OH antibonding σ^* orbital it is clear that this could induce a sensitivity to variations in the intramolecular OH distance. Indeed such a correlation is found, as shown in Fig. 2, where the integrated intensity before the onset is plotted as function of the internal OH1 distance; no correlation was found for either the internal OH2 distance or the H1–O–H2 angle. From the figure we see that the intensity before the onset is nearly linearly dependent on the internal OH1 distance with the highest intensity obtained for the longest distances for which the antibonding orbital is lowest in energy.

The diffraction data are sensitive to the average internal OH distance and the width of the distribution due to zero-point vibrations. However, a reasonable guess of the distribution is required for the fit. In the symmetrical model the two hydrogens are equivalent and are naturally described by

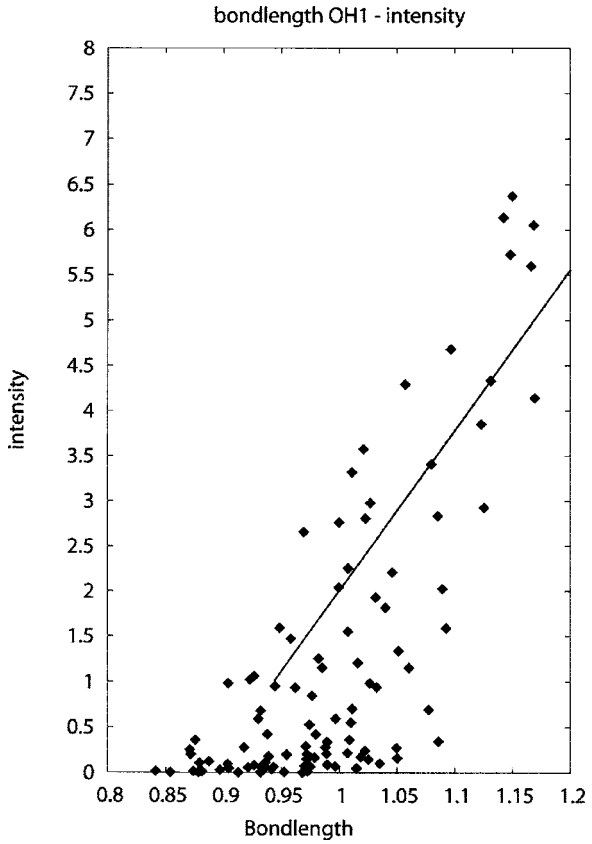

FIG. 2. Correlation between uncoordinated OH1 internal distance and integrated intensity before the preedge for the most asymmetric model. The straight line corresponds to a least-squares fit of points with intensity greater than 1.

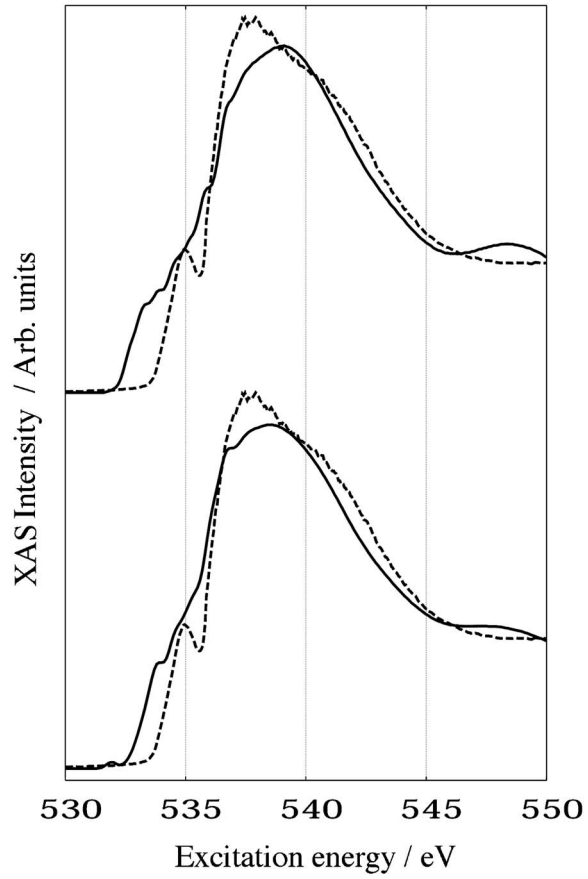

FIG. 3. XA spectra computed for the most asymmetrical model *a*2_6 with (bottom) and without (top) separate vibrational distributions for the H-bonded and non-H-bonded hydrogens.

the same distribution, but in the asymmetrical models this is not a necessary constraint. Indeed, the internal OH distance depends on whether or not it participates in an H-bond and on the strength of this bond. This is seen, e.g., by comparing the OH bond length in gas phase water (0.9572 Å) (Ref. 35) and in ice (≈0.988 Å) (Ref. 43) and is also demonstrated in a recent Compton scattering study comparing ice and liquid water by Nygård *et al.*[44] Furthermore, the OH stretch frequency is redshifted by up to 500 cm^{-1} upon H-bond formation indicative of a less well-defined potential resulting in a broader distribution of OH distances. The distributions of internal OH distances in the gas phase and liquid water have been given by Stern and Berne[45] from simulations including quantum effects using the path integral approach. In the gas phase, comparable to the free OH1 in the asymmetric model, the average bond length from the simulations was 0.9738 Å with a standard deviation of 0.085 Å. In the liquid the width is similar but the average bond length was obtained as 0.999 Å. Adjusting the distribution of internal OH distances according to these considerations to take into account the coordination should thus remove some of the incorrect intensity since the uncoordinated OH1 would be described by a narrower distribution around a shorter average OH1 internal distance.

In Fig. 3 we compare the computed XA spectra for the original *a*2_6 asymmetrical model of Ref. 1 and the modified EPSR fit for the same model, but using two separate internal OH distance distributions for the H-bonded and non-H-bonded OH groups (see the section on methods). This modification removes some of the anomalous intensity before the onset and results in a sharpened structure in this region, but the computed spectrum is still far from the experiment. Interestingly, as shown in Fig. 4, once the dependence on the H-bond situation of the OH distance distributions has been taken into account there is no longer any correlation between the anomalous intensity before the spectrum onset and the non-H-bonded OH1 internal distance. This remaining part of the anomalous intensity before the spectrum onset is thus not due to long internal OH distances but rather due to specific aspects of the environment. By visual inspection of the unoccupied orbitals for several configurations contributing to the intensity before the preedge, it seems possible to make a connection between this anomalous intensity and configurations with hydrogens pointing towards each other, creating pockets which may stabilize the excited state in the DFT XA spectrum calculations similar to what has been concluded for the solvated electron.[46] Furthermore, comparing the spectrum of the *a*2_6 asymmetric model (Fig. 1) with the somewhat less asymmetric model *a*2_4 and the symmetric model, we observe that the onset of the anomalous intensity occurs at higher energy along this sequence, indicating that as the charge on the non-H-bonded hydrogen is increased in the fitting models, the increased repulsion makes it less likely to have these non-H-bonded hydrogens pointing towards each

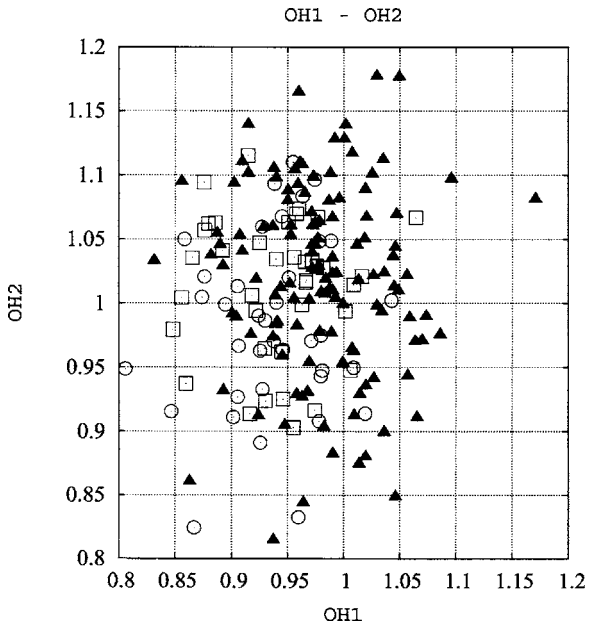

FIG. 4. OH1 and OH2 distances for small (circles), intermediate (squares), and large (triangles) spectrum contributions before the preedge for the most asymmetric model ($a2\_6$) for the case of separate vibrational distributions. The limits have been set at integrated intensities of <0.3 (small), between 0.3 and 0.7 (intermediate), and >0.7 (large).

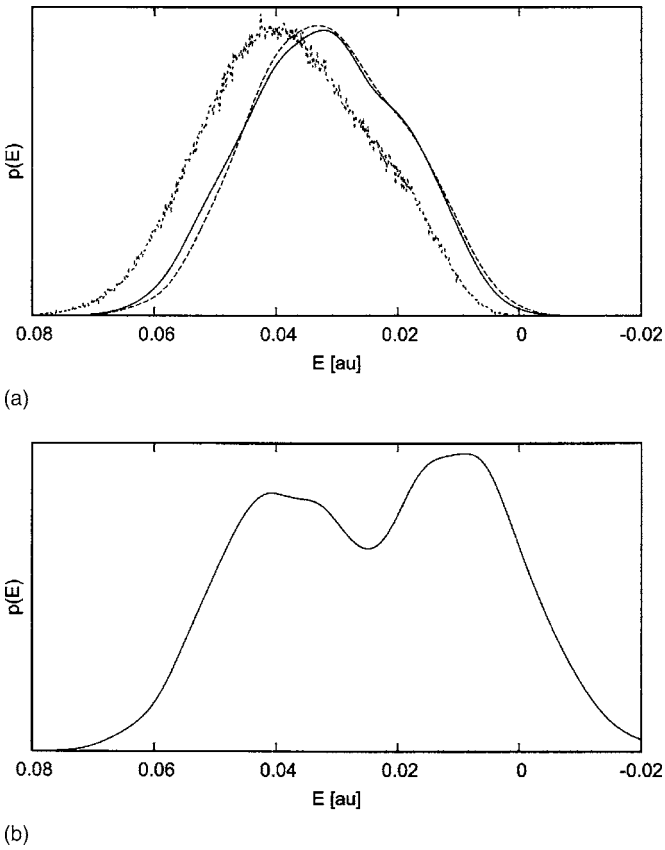

FIG. 5. (a) E-field distributions for symmetric dump using original internal molecular geometries (full line) and SPC/E geometry (dashed) for all molecules. The dotted line peaking at higher E-field shows the E-field distribution from a full SPC/E MD simulation. (b) E-field distributions for the asymmetric $a2\_6$ dump using original molecular geometries. SPC/E charges used throughout.

other. Note that the spectrum calculations at the DFT level involve quantum mechanically determined charge distributions which are different from those assumed in the EPSR fit. Note also that even the symmetrical structural model obtained from the diffraction data shows traces of anomalous intensity before the onset in contrast to symmetrical models obtained from MD simulations.[12]

Let us next turn to the O–H stretch vibrational spectra based on the distribution of the E-fields[5,36,37] or the approach of Hayashi *et al.*[38] using also the field gradients. The symmetric model, based on the E-field approach of Skinner [Fig. 5(a)], gives a distribution with a broad peak centered at approximately 0.035 a.u. and a shoulder at approximately 0.02 a.u.. A positive E-field corresponds to frequencies redshifted relative to gas phase, and as a consequence very little of the distribution should go into the region of negative E-field. The overall shape of the E-field distribution is in qualitative agreement with the experimental Raman spectrum which has been shown to be quantitatively reproduced using SPC/E water and the model (including intensities) of Skinner and co-workers.[5,36,37] In the fitted symmetrical structural model we find that the peak of the E-field distribution is shifted relative to SPC/E water by ~0.008 a.u. towards a lower E-field, indicating that the symmetrical model from the diffraction data does not produce a Raman spectrum peaking at the correct frequency. From the linear relationship we estimate a discrepancy close to 100 cm^{-1}, i.e., similar to the shift between ice and liquid water. This is not due to the flexibility of the molecules in the EPSR fit since changing the internal geometry of the molecules to SPC/E geometry has only minor effects shifting the distribution to a somewhat lower E-field, corresponding to an additional small blueshift of the uncoupled frequency, while leaving the overall shape of the distribution almost intact. The change in molecular geometry from that obtained from the fit to the diffraction data to the SPC/E geometry thus has only a small effect on the E-field distribution.

The approach of Hayashi *et al.* gives for the symmetric model an IR spectrum [Fig. 6(a)] which in shape is rather similar to the E-field distribution of Fig. 5(a) (representing the Raman spectrum). Note that the intensity of the higher frequency vibrations becomes scaled down when converting the underlying fields and gradients to an IR spectrum. This affects the comparison at higher frequency (lower E-field) somewhat. However, for the symmetric model both approaches are in basic agreement and give a reasonable representation of the shape of the experimental spectrum with the Skinner model giving seemingly better agreement. The comparison between the predicted IR spectra from the symmetrical model $a2$ and a full SPC/E MD simulation in Fig. 6(a) confirms the observation from Fig. 5(a) that the vibrational spectrum for the present symmetrical solution is significantly blueshifted compared with SPC/E and experiment; this is furthermore consistent with the lower H-bond count (2.9) in this symmetric structure model compared to SPC/E (3.5).

For the most asymmetric model, on the other hand, the two approaches give strongly different results [Figs. 5(b) and 6(b)]. The E-field distribution [Fig. 5(b)] looks radically dif-

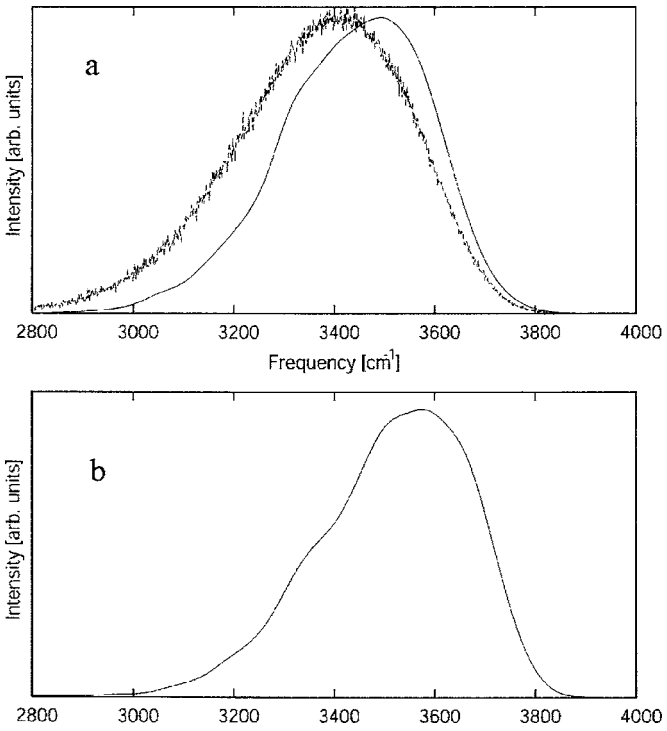

FIG. 6. Predicted IR spectra using the method of Hayashi *et al.* for (a) the symmetric ($a2$) structure (full line) and for SPC/E MD simulation (noisy line). (b) The most asymmetric $a2\_6$ structural solution.

ferent from the symmetric case reflecting the bimodal bonding situation (with roughly half of the hydrogens involved in H-bonds) as two distinct peaks in the E-field distribution, one centered at ~0.045 a.u. and the other at ~0.005 a.u. corresponding to H-bonded and free hydrogens, respectively. As in the symmetric case, a change in internal geometry induces only a small change in the E-field distribution (not shown).

Extrapolating the linear relationship between E-field and frequency as given by Skinner and co-workers,[36,37] a negative E-field would correspond to frequencies higher than the gas phase frequency. In order to investigate whether this approximate relationship holds for negative E-fields, the frequencies were computed quantum mechanically following the procedure and basis sets of Ref. 36 and 37 using cluster models of the corresponding structures. Sampling structures with strongly negative E-fields, we indeed find that these correspond to unphysical frequencies strongly increased over the gas phase as predicted by extrapolating the linear relationship. The most extreme cases were found to correspond to situations where two nominally uncharged hydrogens were in close proximity to each other. These situations with strongly blueshifted vibrational frequencies must be excluded based on their contributions to the Raman spectrum although they seem to be allowed by the diffraction data.

From Fig. 6(b), however, we see that the model, including also the field gradients, gives a completely different prediction for the spectrum of the asymmetric model. We no longer find a bimodal distribution, but rather a spectrum of similar shape as the symmetric model, but shifted towards higher frequencies. In Figs. 7 and 8 we show the contributions from the individual OH-stretches for the two approaches applied to the two models [asymmetric model: OH1 (free) and OH2 (H-bonded)]. The approach of Skinner and co-workers predicts a strong redshift of the H-bonded OH2 stretch in the asymmetric model compared to the H-bonded stretch in the symmetrical model. In contrast to this a slight blueshift is predicted for the H-bonded component in the asymmetrical case when the field gradients are included (Fig. 8). Both approaches agree on a blueshift of the non-H-bonded stretch although the magnitude would seem to be different. It should be noted that in Fig. 8 the contributions to the spectrum from the two OH stretches are shown, where the higher frequency mode is scaled down in intensity due to the conversion of the underlying fields and gradients into intensity. In Fig. 7, on the other hand, we only report the distribution of E-fields projected along the intramolecular OH-bonds without considering their relative intensities.

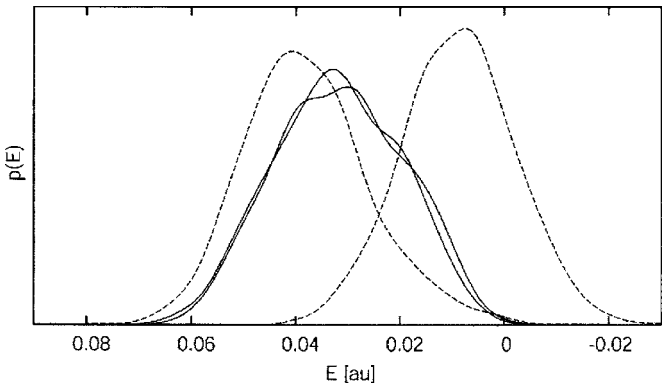

FIG. 7. Contributions from individual (OH1 and OH2) stretches according to the model of Skinner and co-workers. Symmetrical model in full lines and asymmetrical in dotted lines with the non-H-bonded OH at lower E-field.

To summarize, we find qualitative agreement between the two different approaches for the symmetric model, but strongly different predictions for the asymmetric structure, making it difficult to draw any firm conclusions. We note that both Skinner and co-workers and Hayashi *et al.* have fitted their models based on structures obtained from MD simulations in which asymmetrical situations are very rare.[13] Since these situations are under-represented in the respective training sets, this may lead to larger uncertainties in these cases.

In order to calibrate the performance of the respective

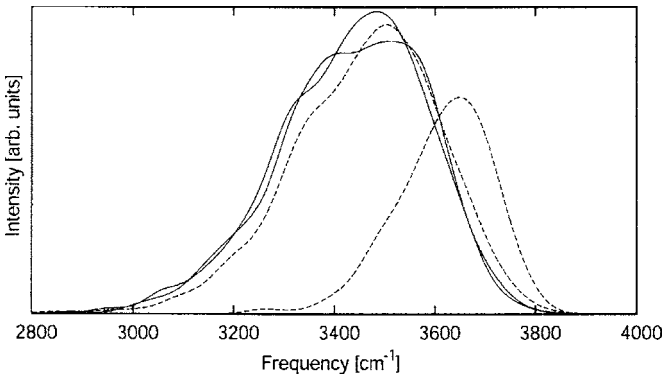

FIG. 8. Contributions from individual (OH1 and OH2) stretches according to the model of Hayashi *et al.* Symmetrical model in full lines and asymmetrical in dotted lines with the non-H-bonded OH at higher frequency.

models in comparison with a fully coupled anharmonic calculation, we have used an isolated water ring-hexamer and a water ditetramer which were possible to geometry optimize at the B3LYP/6-311++G(d,p) level. This calibration cannot be performed on general structures from MD since the full anharmonic *ab initio* calculation must be performed at the energy minimum of the structure. The anharmonic frequencies were calculated at the same level of theory using the method of Barone[40] for an HOD in D_2O, with the H either H-bonded or free. The resulting frequencies were 3696 and 3235 cm^{-1} for, respectively, the free and H-bonded OH stretches in the hexamer and 3271 cm^{-1} for the symmetrically H-bonded molecule in the ditetramer. The corresponding frequencies assuming no coupling and only moving the OH of interest to obtain eight points along the OH-stretch for the fit to a Morse potential, as suggested by Skinner and co-workers,[36,37] become 3779, 3133, and 3194 cm^{-1}. The free OH stretch is thus overestimated (blueshifted) by 83 cm^{-1} while the H-bonded one is underestimated (redshifted) by 102 cm^{-1} for the hexamer and by 77 cm^{-1} for the symmetrical H-bond in the ditetramer. Nondiagonal couplings (between different normal modes) lower the non-H-bonded frequency by 25 cm^{-1} and increase the H-bonded one by 57 and 45 cm^{-1} for the hexamer and ditetramer, respectively. The remaining difference is mainly due to differences in the description of the harmonic frequency which is sensitive to the step size used in fitting the Morse potential, and this effect seems to be larger for free OH:s than for bonded ones. The OH-stretch in gas phase HOD computed with the same technique and using the suggested method of Skinner fitting a Morse potential to eight computed points with 0.08 Å separation becomes 3763 cm^{-1}. Changing the step size to 0.04 Å results in a frequency of 3706 cm^{-1}, while the method of Barone gives 3686 cm^{-1} (including an intermode coupling of −21 cm^{-1}) to be compared with the experimental value of 3707 cm^{-1};[47] the low value compared to experiment is expected since the B3LYP functional is known to underestimate vibrational frequencies for water as seen from comparison with MP2.[48] Note that in all cases above the comparison is between two quantum chemical calculations using the same level of theory and both including anharmonicity, but with an assumption of no coupling and an approximation of a Morse potential in the approach of Skinner and co-workers. In summary, this approach tends to strongly overestimate the redshift of the H-bonded stretch and give a blueshift of the free OH-stretch resulting in an exaggerated separation by more than 100 cm^{-1} of the two classes of contributions in the asymmetric structural model.

Applying the model of Hayashi *et al.*, on the other hand, using the fields and field gradients generated by assuming SPC/E charges for the remaining molecules in the hexamer ring we obtain 3675 and 3330 cm^{-1}, respectively. In this approach the non-H-bonded OH stretch is redshifted by 34 cm^{-1} compared to the reference calculation. The H-bonded stretch, on the other hand, is blueshifted by 97 cm^{-1} with respect to the full calculation. In contrast to what was found for the approach by Skinner we thus find a compression of the spectrum when applying the approach of Hayashi *et al.* Both methods thus seem to have difficulties representing the width of the spectrum which becomes particularly evident with two classes of contributions: the approach of Skinner strongly exaggerates the separation of H-bonded and non-H-bonded contributions while that of Hayashi *et al.* instead leads to a compressed predicted spectrum. In addition, it has to be noted that the latter method is quite sensitive to the point charges used.

DISCUSSION

To what extent are the present experimental XAS and XRS data and their interpretation reliable? This is a relevant initial question before using them together with well-established x-ray and neutron diffraction techniques as well as IR/Raman data to evaluate different structural models of water. XAS on liquid water using fluorescence detection requires correction for saturation effects as indicated in Ref. 13 and 41 and discussed extensively by Näslund *et al.*[6] XRS, as a hard x-ray energy-loss technique, intrinsically has no saturation effects. Possible non-dipole contributions have been discussed in the supplementary material of Ref. 13 and shown to be negligible at the low Q-transfers used in that work. XAS measured in transmission mode is free of both effects, but can only be performed on a thin liquid sample due to the short penetration depth of soft x-rays. A comparison of these three bulk sensitive, photon-in/photon-out techniques to record the core-excitation spectrum of the liquid shows very consistent, stable, and reliable spectra establishing the accuracy of the experimental data.[6]

As discussed in the introduction the interpretation of the experimental data has been questioned by several workers. Smith *et al.*[2] used electron yield XAS on a liquid microjet to estimate the energy difference between SD and DD species. Their spectra and analysis were, however, criticized in a technical comment by Nilsson *et al.*[3] Fernandez-Serra and Artacho[11] used molecular dynamics to suggest that a "flapping motion" of the H-bond-accepting molecule could lead to the observed preedge feature even in tetrahedral coordination. The XA spectra were never calculated, however, and instead the p-characters of the LUMO and LUMO+1 orbitals of the ground state were used to represent the ratio of preedge to main-edge intensity. Since many states contribute to the main edge, this procedure becomes completely arbitrary and has no connection with the XA spectrum. It is furthermore well known that ground state orbitals are not appropriate to describe XAS.[49]

A fundamental prerequisite for the present study is that the x-ray absorption spectrum calculations are sufficiently accurate. This has been demonstrated for well-defined gas phase molecules,[25,27,42] metal complexes,[50] the periodic overlayer of n-octane on Cu(110),[51] the water contact layer on Pt(111),[52] as well as for specific H-bonded systems with known structure such as bulk and surface of ice,[13] bulk methanol,[53] and the ordered (3×2) periodic overlayer of glycine on Cu(110).[54] The agreement with experiment is, in all cases, very good. For liquid water, calibration calculations comparing with experiment are more difficult since the structure is unknown. However, for general structures taken from CPMD simulations,[55] a fully periodic plane-wave calculation

of the XA spectra is in complete agreement with the localized basis set cluster model calculation of the same structure once the unit cell and cluster sizes are large enough.[56] The computational technique has been discussed by Cavalleri *et al.*[7] with specific reference to calculations on water. For liquid water we have furthermore demonstrated that, although the original cone criterion of Wernet *et al.*[13] fails to predict the liquid water spectrum when applied to general structures, it is possible to obtain qualitative agreement with the XA experiment with the present computational approach by additionally restricting the cone criterion to even more strongly asymmetric configurations from the CPMD trajectories.[12] This therefore provides additional theoretical support for the recent claims based on experimental comparisons of bulk and surface of ice that the local order in water is strongly asymmetric.[3,13,41] Other sources,[2,9,57] however, claim to be able to reach agreement with the XA spectrum also for quasi-tetrahedrally H-bonded water. Arguments against this have been given,[3,7] but at the present time some controversy still remains.

Given the present asymmetric model, which reproduces the hydrogen bond numbers proposed by Wernet *et al.* but still does a poor job at reproducing the XA spectrum, and given that changing the water molecule geometry with an imperceptible change in the intermolecular structure produces a marked change in the calculated XA spectrum, it is interesting to note the sharpness of the preedge feature in the experimental XA spectrum of the liquid. This is in accordance with the observation that the only way found so far to obtain agreement between the calculated XA spectrum and the XA data is to apply a more restrictive cone criterion to extract highly asymmetric configurations from the CPMD simulation, indicative of some limited range of structures contributing to the preedge region.[9] However, as concluded in Ref. 9 it also implies that other factors in addition to the local water symmetry are responsible for the shape of the XA spectrum. It furthermore has to be said that finding a water structure that reproduces the XA spectrum, or any other observable, is no guarantee that it is the only structure that will achieve this fit, nor that it is necessarily the correct structure, as the results of EPSR refinement of the diffraction data in Ref. 1 have shown only too clearly. The present EPSR fitted models contain a significant fraction of water molecules with H atoms pointing towards each other on neighboring molecules, in particular, in the case of the asymmetric potential models due to the only weakly charged or neutral H atoms, but also to a much lesser extent in the symmetrical case. These structures are not expected to occur with any frequency based on simple considerations of H-bonding, but apparently the diffraction data by itself were insufficient to exclude such situations.

In the present work a hydrogen bond is defined according to the XA spectrum-related cone-criterion of Wernet *et al.*[13] This gives an H-bond number of 2.9 for the present symmetric model and an H-bond number of 2.2 for the fully asymmetric model. Interestingly, both of these numbers are smaller than the ~3.5 H bonds found in, e.g., SPC/E water using the same criterion. The H-bond statistics in the asymmetric situation are similar to what was concluded by Wernet *et al.* although we note that later work treating more general, disordered structures has resulted in an even more restrictive connection between spectral features and structure: a sufficient criterion for a good computed representation of the XA spectrum from general structures is thus that the intact H-bond should be within a small cone with O–O distance at least shorter than 2.9 Å, while the distorted bond should be significantly distorted.[12] In the present case we find that the studied models show discrepancies with the XAS experiment even when asymmetry is included. Based on the XA spectrum calculations we have introduced intramolecular constraints in the fitting of the diffraction data which improves the predicted XA spectrum somewhat, but which still does not lead to a satisfactory representation of the liquid water XA spectrum.

It has been shown previously by Skinner and co-workers that the E-field distribution based on the SPC/E classical force-field model generates a line shape close to the experimental OH stretch Raman spectrum of HOD in D_2O.[36,37] Since the symmetrical model from SPC/E simulations gives an E-field distribution similar to experiment, this has been taken to indicate support for the symmetrical model and that other models must be excluded.[5] In the present work we find that application of the approach of Skinner *et al.* to the asymmetrical structures from the EPSR fits leads to a strongly bimodal distribution, which does not resemble the experimental spectrum. However, application of the approach of Hayashi *et al.*,[38] including also the electric field gradients in the parametrization, leads to a totally different result with a single broad distribution in qualitative agreement with experiment, however, somewhat blueshifted. It is thus unclear what conclusions can be drawn from this. Our *ab initio* anharmonic calculations of the gas phase hexamer and ditetramer indicate that the approach of Skinner and co-workers overestimates the redshift of the H-bonded OH-stretch, while it gives a too high frequency for the non-H-bonded stretch. This artifact contributes strongly to the bimodal character of the obtained spectrum in the asymmetric case. On the other hand, in the approach of Hayashi *et al.* both the redshift of the H-bonded stretch and the blueshift of the free OH are underestimated. That both approaches lead to qualitatively equivalent descriptions of the vibrational spectra of the symmetric model may possibly be taken as indicative of the method used to determine the parameters in each approach, i.e., using structures obtained from MD simulations. Since these contain asymmetric structural motifs only to a vanishing extent, the respective parametrizations in these situations might be less reliable than for the more frequent symmetric cases.

Turning to experiment we note that the anti-Stokes Raman measurements by Dlott and co-workers[58] indicate two distinguishable subbands, one redshifted and the other blueshifted, supporting a two-component model of water. The results could thus be interpreted as a bimodal distribution with two distinct OH stretch vibrations supporting an asymmetrical model but can also be related to different species. The relative intensity of the two subbands showed nearly an order of magnitude difference between the OH stretch in HOD and H_2O, demonstrating the complexity of the spectro-

scopic vibrational process. It is clear that more understanding regarding the OH vibrational spectral line shape, vibrational coupling, spectral diffusion, and intensity is necessary before firm conclusions can be drawn regarding the validity of different water models using Raman and IR spectra.

Based on all three experimental probes, what can we currently say regarding the two different classes of water models, symmetrical or asymmetrical? It is clear that the present EPSR analysis of the diffraction data as stated in Ref. 1 is inconclusive and does not make a strong distinction between symmetrical and asymmetrical models. The specific features in the XA spectrum of liquid water, on the other hand, have been shown, through model experiments on the surface of ice and spectrum calculations, to be due to an asymmetric local coordination with one strong and one weak donating H bond.[12,13,41] Smith *et al.*[5] have, on the other hand, used the connection between E-field and frequency[59] to demonstrate that the E-field distributions from their Monte Carlo simulations using the SPC/E force field closely mimic also the temperature dependence in the IR and Raman spectra of water which, under the assumption of weak intermode coupling and a 1:1 E-field to intensity relationship, would support a symmetrical model but not exclude all alternative models, since other models have not been tested, and furthermore the reliability of predicted spectra for more distorted models is unclear. At the moment we cannot draw any strong conclusion from Raman or IR measurement, and it is necessary to investigate the OH-stretch region further with new experimental and theoretical approaches. Until then it will be important to obtain a full agreement between diffraction data and XAS using other possible water structures.

CONCLUSIONS

In the present work we have analyzed the different models of the liquid water structure obtained in Ref. 1 from fits to available neutron and x-ray diffraction data in terms of their ability to also reproduce the XA and IR/Raman spectra of liquid water. The models can be classified as symmetric and asymmetric with varying degree of asymmetry as obtained by removing the usual assumption of equal charges on the two hydrogens in the EPSR fit to the diffraction data. Although all models could be made to represent the diffraction data to an equal goodness of fit, we find that neither of the thus fitted structures is able to reproduce the experimental XA spectrum of liquid water, nor accurately the IR and Raman spectra. As previously discussed,[12,13] the symmetrical model results in an ice-like XA spectrum with too low intensity in the preedge and main-edge regions and the postedge at too low energy. Introducing separate internal OH distance distributions for the H-bonded and non-H-bonded hydrogens in the most asymmetrical model ($a2\_6$) improves the representation of the XA spectrum and shows correct intensity but wrong spectral shape in the preedge region, and the model thus still does not catch the essential features of the experimental liquid water XA spectrum. We have earlier shown, however, that a more restrictive cone criterion applied to select structures from CPMD simulations for the spectrum calculations can produce an average XA spectrum resembling the experiment within the present computational approach.[12] We thus conclude that, although the local coordination in terms of the number of H-bonds is similar between the asymmetric models studied in the present work and that of Ref. 13, there are still significant differences between the models in terms of the XA spectroscopy. Specifically, the low charge on the non-H-bonded hydrogen used to generate the present asymmetrical structure models has resulted in the occurrence of structures where these hydrogens are in close proximity of each other. This furthermore shows that, in spite of the use of experimental x-ray diffraction data in combination with neutron diffraction data from five isotope mixtures, the assumed potential still has a strong influence on the resulting structure. The actual charge distribution in the DFT spectrum calculations on the structures with hydrogen-hydrogen interaction leads to a stabilization of the excited electron and computed intensity before the onset of the experimental spectrum. We can view this as the preedge spectral feature has been shifted further downwards in energy and inhomogeneously broadened due to these additional interactions.

The electric field projected along the internal O–H bond has been used as a predictor of the vibrational frequency for the OH(OD) stretch of HOD in $D_2O(H_2O)$ by Skinner and co-workers[36,37] and Smith *et al.*[5] under the assumption of negligible intermode coupling. The E-field distribution from the symmetrical model is similar to the Raman spectrum of the isotope-substituted liquid, while the asymmetrical models using this approach result in a bimodal distribution due to the two distinct classes of H-bonded and non-H-bonded OH groups in the model. However, using instead the parametrization of Hayashi *et al.*,[38] we obtain a very different spectrum not showing any bimodality. We find that the approach of Skinner and co-workers enhances the separation of H-bonded and non-H-bonded contributions, while that of Hayashi *et al.* leads to a compressed spectrum. It is thus not clear to us at the present time what the correct representation of the vibrational spectra of water models based on the structure should be. We note that in neither approach explicitly asymmetric situations have been considered in the determination of the required parameters but also that recent studies using pump-probe anti-Stokes Raman measurements by Dlott *et al.*[58] show two distinct components indicating a bimodal distribution.

In conclusion, we observe that the structures we have investigated in the present work were obtained from Ref. 1 where they were generated by fitting D_2O and H_2O neutron diffraction data in combination with the x-ray diffraction data from Hura *et al.*[18] from 2000. We find that neither the fitted symmetric nor asymmetric model fits the XAS or IR/Raman spectroscopic data. Since, assuming the validity of the E-field representation of IR/Raman data in the symmetrical case, the fitted symmetrical model gives a significantly blueshifted spectrum compared with experiment as well as the observation that the structures fitted to the present diffraction data reflect the assumed potential model, it is likely that more extended x-ray diffraction measurements on liquid water are needed. We conclude that the present approach to combine the fit to the diffraction data with the recent XAS

data as well as IR/Raman spectra through an integrated, iterative process holds promise, but it is likely that improved x-ray diffraction data and models to predict IR/Raman spectra based on structure are needed if more conclusive results on the water structure are to be obtained.

ACKNOWLEDGMENTS

The authors thank A. K. Soper for supplying the structures, for extensive comments on the manuscript, and for performing the EPSR fits in the present work and J. Skinner, S. Brennan, and S. Mukamel for discussions and helpful comments. This work was supported by the Swedish Foundation for Strategic Research, the Swedish Research Council (VR), and the National Science Foundation (U.S.) CHE-0518637. Portions of this research were carried out at the Stanford Synchrotron Radiation Laboratory, a national user facility operated by Stanford University on behalf of the U.S. Department of Energy, Office of Basic Energy Sciences.

[1] A. K. Soper, J. Phys.: Condens. Matter **17**, S3273 (2005).
[2] J. D. Smith, C. D. Cappa, K. R. Wilson, B. M. Messer, R. C. Cohen, and R. J. Saykally, Science **306**, 851 (2004).
[3] A. Nilsson, Ph. Wernet, D. Nordlund *et al.*, Science **308**, 793a (2005).
[4] Y. A. Mantz, B. Chen, and G. J. Martyna, Chem. Phys. Lett. **405**, 294 (2005).
[5] J. D. Smith, C. D. Cappa, K. R. Wilson, R. C. Cohen, P. L. Geissler, and R. J. Saykally, Proc. Natl. Acad. Sci. U.S.A. **102**, 14171 (2005).
[6] L. Å. Näslund, J. Lüning, Y. Ufuktepe, H. Ogasawara, Ph. Wernet, U. Bergmann, L. G. M. Pettersson, and A. Nilsson, J. Phys. Chem. B **109**, 13835 (2005).
[7] M. Cavalleri, D. Nordlund, M. Odelius, A. Nilsson, and L. G. M. Pettersson, Phys. Chem. Chem. Phys. **7**, 2854 (2005).
[8] D. Prendergast, J. C. Grossman, and G. Galli, J. Chem. Phys. **123**, 014501 (2005); Y. A. Mantz, B. Chen, and G. J. Martyna, J. Phys. Chem. B **110**, 3540 (2006).
[9] D. Prendergast and G. Galli, Phys. Rev. Lett. **96**, 215502 (2006).
[10] T. Head-Gordon and M. E. Johnson, Proc. Natl. Acad. Sci. U.S.A. **103**, 7973 (2006).
[11] M. V. Fernandez-Serra and E. Artacho, Phys. Rev. Lett. **96**, 016404 (2006).
[12] M. Odelius, M. Cavalleri, A. Nilsson, and L. G. M. Pettersson, Phys. Rev. B **73**, 024205 (2006).
[13] Ph. Wernet, D. Nordlund, U. Bergmann *et al.*, Science **304**(5673), 995 (2004).
[14] J. D. Bernal and R. H. Fowler, J. Chem. Phys. **1**, 515 (1933).
[15] A. H. Narten and H. A. Levy, Science **165**, 447 (1969).
[16] A. Rahman and F. H. Stillinger, J. Chem. Phys. **55**, 3336 (1971).
[17] B. Guillot, J. Mol. Liq. **101**, 219 (2003).
[18] G. Hura, J. M. Sorenson, R. M. Glaeser, and T. Head-Gordon, J. Chem. Phys. **113**, 9140 (2000).
[19] J. M. Sorenson, G. Hura, R. M. Glaeser, and T. Head-Gordon, J. Chem. Phys. **113**, 9149 (2000).
[20] T. Head-Gordon and M. E. Johnson, Proc. Natl. Acad. Sci. U.S.A. **103**, 16614 (2006).
[21] L. Fu, S. Brennan, and A. Bienenstock (unpublished).
[22] T. Todorova, A. P. Seitsonen, J. Hutter, I.-F. W. Kuo, and C. J. Mundy, J. Phys. Chem. B **110**, 3685 (2006); J. Vandevondele, F. Mohamed, M. Krack, J. Hutter, M. Sprik, and M. Parrinello, J. Chem. Phys. **122**, 014515 (2005); J. C. Grossman, E. Schwegler, E. W. Draeger, F. Gygi, and G. Galli, *ibid.* **120**, 300 (2004); E. Schwegler, J. C. Grossman, F. Gygi, and G. Galli, *ibid.* **121**, 5400 (2004).
[23] B. Chen, I. Ivanov, M. L. Klein, and M. Parrinello, Phys. Rev. Lett. **91**, 215503 (2003).
[24] K. Hermann, L. G. M. Pettersson, M. E. Casida *et al.*, STOBE software, 2005.
[25] L. Triguero, L. G. M. Pettersson, and H. Ågren, Phys. Rev. B **58**, 8097 (1998).
[26] H. Ågren, V. Carravetta, O. Vahtras, and L. G. M. Pettersson, Theor. Chem. Acc. **97**, 14 (1997).
[27] C. Kolczewski, R. Püttner, O. Plashkevych *et al.*, J. Chem. Phys. **115**, 6426 (2001).
[28] S. Huzinaga, J. Chem. Phys. **42**, 1293 (1965).
[29] W. Kutzelnigg, U. Fleischer, and M. Schindler, *NMR-Basic Principles and Progress* (Springer, Heidelberg, 1990).
[30] L. G. M. Pettersson, U. Wahlgren, and O. Gropen, J. Chem. Phys. **86**, 2176 (1987).
[31] A. D. Becke, Phys. Rev. A **38**, 3098 (1988).
[32] J. P. Perdew, Phys. Rev. B **33**, 8822 (1986).
[33] O. Takahashi and L. G. M. Pettersson, J. Chem. Phys. **121**, 10339 (2004).
[34] R. Sankari, M. Ehara, H. Nakatsuji, Y. Senba, K. Hosokawa, H. Tyoshida, A. De Fanis, Y. Tamenori, S. Aksela, and K. Ueda, Chem. Phys. Lett. **380**, 647 (2003).
[35] W. S. Benedict, N. Gailar, and E. K. Phylar, J. Chem. Phys. **24**, 1139 (1956).
[36] S. A. Corcelli, C. P. Lawrence, and J. L. Skinner, J. Chem. Phys. **120**, 8107 (2004).
[37] S. A. Corcelli and J. L. Skinner, J. Phys. Chem. A **109**, 6154 (2005).
[38] T. Hayashi, T. Jansen, W. Zhuang, and S. Mukamel, J. Phys. Chem. A **109**, 64 (2005).
[39] M. J. Frisch, G. W. Trucks, H. B. Schlegel *et al.*, GAUSSIAN 98 Gaussian Inc., Pittsburgh, PA, 1998.
[40] V. Barone, J. Chem. Phys. **122**, 104108 (2005).
[41] S. Myneni, Y. Luo, L. Å. Näslund *et al.*, J. Phys.: Condens. Matter **14**, L213 (2002).
[42] M. Cavalleri, H. Ogasawara, L. G. M. Pettersson, and A. Nilsson, Chem. Phys. Lett. **364**, 363 (2002).
[43] W. F. Kuhs and M. S. Lehmann, J. Phys. Colloq. **C1**, 3 (1987).
[44] K. Nygård, M. Hakala, S. Manninen, A. Andrejczuk, M. Itou, Y. Sakurai, L. G. M. Pettersson, and K. Hämäläinen, Phys. Rev. E **74**, 031503 (2006).
[45] H. A. Stern and B. J. Berne, J. Chem. Phys. **115**, 7622 (2001).
[46] K. S. Kim, I. Park, S. Lee, K. Cho, J. Y. Lee, J. Kim, and J. D. Joannopoulos, Phys. Rev. Lett. **76**, 956 (1996); L. Kevan, Acc. Chem. Res. **14**, 138 (1981).
[47] T. Shimanouchi, Report No. NSRDS-NBS 39, 1972.
[48] K. Diri, E. M. Myshakin, and K. D. Jordan, J. Phys. Chem. A **109**, 4005 (2005).
[49] J. Stöhr, *NEXAFS Spectroscopy* (Springer-Verlag, Berlin, 1992).
[50] L. G. M. Pettersson, T. Hatsui, and N. Kosugi, Chem. Phys. Lett. **311**, 299 (1999); R. G. Wilks, J. B. Macnaughton, H. B. Kraatz, T. Regier, and A. Moewes, J. Phys. Chem. B **110**, 5955 (2006).
[51] H. Öström, L. Triguero, K. Weiss, H. Ogasawara, M. G. Garnier, D. Nordlund, M. Nyberg, L. G. M. Pettersson, and A. Nilsson, J. Chem. Phys. **118**, 3782 (2004); K. Weiss, H. Öström, L. Triguero, H. Ogasawara, M. G. Garnier, L. G. M. Pettersson, and A. Nilsson, J. Electron Spectrosc. Relat. Phenom. **128**, 179 (2003).
[52] H. Ogasawara, B. Brena, D. Nordlund, M. Nyberg, A. Pelmenschikov, L. G. M. Pettersson, and A. Nilsson, Phys. Rev. Lett. **89**, 276102 (2002).
[53] K. R. Wilson, B. S. Rude, R. D. Schaller, T. Catalano, R. J. Saykally, M. Cavalleri, A. Nilsson, and L. G. M. Pettersson, J. Phys. Chem. B **109**, 10194 (2005).
[54] M. Nyberg, M. Odelius, A. Nilsson, and L. G. M. Pettersson, J. Chem. Phys. **119**, 12577 (2003).
[55] R. Car and M. Parrinello, Phys. Rev. Lett. **55**, 2471 (1985).
[56] M. Cavalleri, M. Odelius, A. Nilsson, and L. G. M. Pettersson, J. Chem. Phys. **121**, 10065 (2004).
[57] B. Hetenyi, F. De Angelis, P. Gianozzi, and R. Car, J. Chem. Phys. **120**, 8632 (2004).
[58] J. C. Deak, S. T. Rhea, L. K. Iwaki, and D. D. Dlott, J. Phys. Chem. A **104**, 4866 (2000); Z. Wang, A. Pakoulev, Y. Pang, and D. D. Dlott, *ibid.* **108**, 9054 (2004).
[59] C. J. Fecko, J.. D. Eaves, J. J. Loparo, A. Tokmakoff, and P. L. Geissler, Science **301**, 1698 (2003).